Diode-Laser-Based Direct-Detection Doppler Wind Lidar

Luke Colberg
Advisor: Kevin Repasky

Electrical and Computer Engineering
Montana State University

March 7th, 2024

lukecolberg@montana.edu

Table of Contents

Observational Needs for Weather Forecasting

Observational Needs for Weather Forecasting

- In atmospheric science, the wind field describes the motion of air masses.

Observational Needs for Weather Forecasting

- In atmospheric science, the wind field describes the motion of air masses.
- Wind speed and direction measurements are necessary to support weather forecasting and other fields within atmospheric science.

Observational Needs for Weather Forecasting

- In atmospheric science, the wind field describes the motion of air masses.
- Wind speed and direction measurements are necessary to support weather forecasting and other fields within atmospheric science.

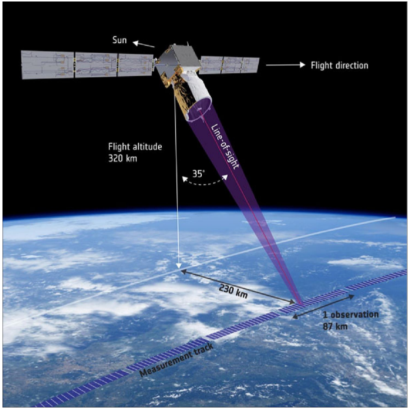

ADM-Aeolus Satellite (image credit: European Space Agency)

Observational Gaps

Observational Gaps

- Wind measurements are especially important within the lower free troposphere and the Planetary Boundary Layer (PBL).

- Wind measurements are especially important within the lower free troposphere and the Planetary Boundary Layer (PBL).

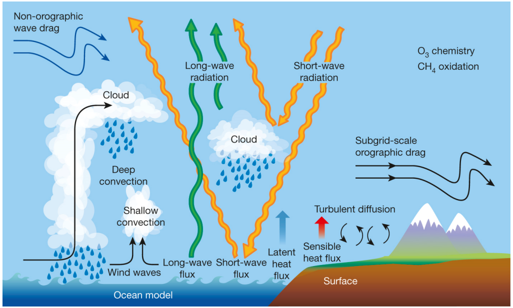

P. Bauer et al. Nature 525, 47-55 (2015) doi:10.1038/nature14956

Observational Gaps

- Wind measurements are especially important within the lower free troposphere and the Planetary Boundary Layer (PBL).
- Better observations of wind speeds in this region would benefit weather forecasting, climate modeling, and various other applications.

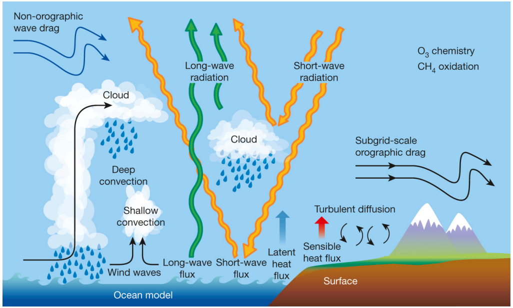

P. Bauer et al. Nature 525, 47-55 (2015) doi:10.1038/nature14956

Doppler Wind Lidar

Doppler Wind Lidar

- **Doppler Wind Lidar (DWL)** provide continuous high-resolution wind speed profiles in clear conditions.

Doppler Wind Lidar

- **Doppler Wind Lidar (DWL)** provide continuous high-resolution wind speed profiles in clear conditions.

- These instruments emit light at frequency f_0 and detect light at a Doppler-shifted frequency $f_0 + \Delta f$

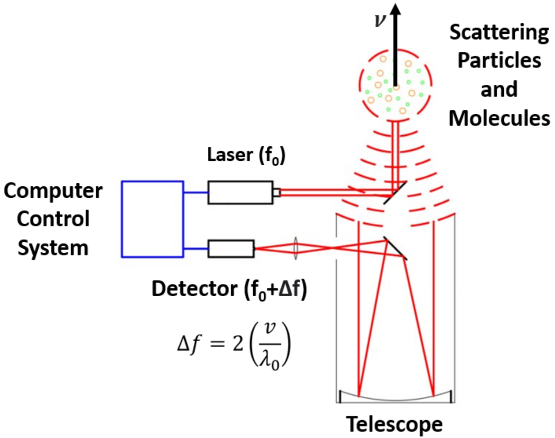

Two-Component Atmosphere

Two-Component Atmosphere

The scattering spectrum from molecules ($\sim$ 2 GHz) is much broader than from aerosols ($\sim$ 2 MHz).

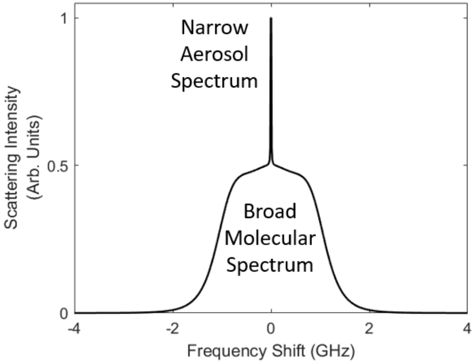

Two-Component Atmosphere

Definition

B is the backscatter ratio. It is the ratio of the total atmospheric scattering to the component of scattering that comes from molecules.

$$\mathrm{B}(\mathrm{r}) = \frac{\beta_{\mathrm{m}}(\mathrm{r}) \ + \beta_{\mathrm{a}}(\mathrm{r})}{\beta_{\mathrm{m}}(\mathrm{r})}$$

Two-Component Atmosphere

The scattering spectrum from molecules ($\sim$ 2 GHz) is much broader than from aerosols ($\sim$ 2 MHz).

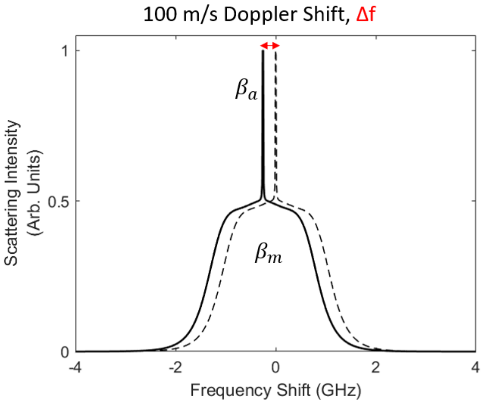

Doppler Wind Lidar Measurement Techniques

DWL Technology	Example Instrument/ Lead	Signal	Wavelength
Filter	TWiLiTE/ NASA Goddard (U.S.A.)	Aerosols + Molecular	355 nm
	OHP Lidar/ CNRS (France)	Aerosols + Molecular	532 nm
Interferometric	OAWL/ Ball (U.S.A.)	Aerosols/Molecular	355, 532, 1064 nm
	HALAS/ Honeywell (U.S.A.)	Aerosols/Molecular	355 nm
Heterodyne	WindCube/ Vaisala-Leosphere (France)	Aerosols	1.543 µm
	DAWN/ NASA Langley (U.S.A.)	Aerosols	2.053 µm

Previous Work: The MicroPulse Differential Absorption Lidar (MPD)

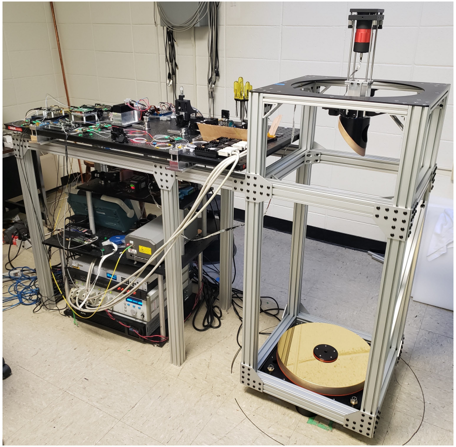

MPD instrument at MSU.

- The MPD's diode-laser-based design is **cost-effective** and enables **eye-safe** operation with a class 1M designation.

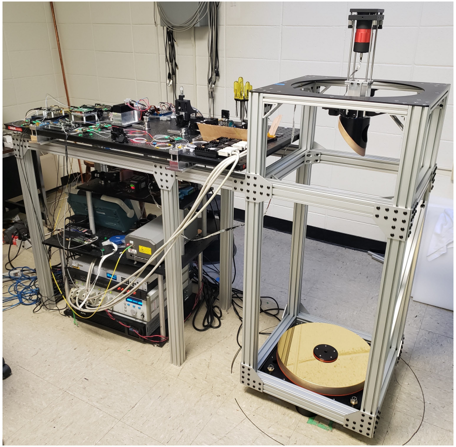

MPD instrument at MSU.

Previous Work: The MicroPulse Differential Absorption Lidar (MPD)

- The MPD's diode-laser-based design is **cost-effective** and enables **eye-safe** operation with a class 1M designation.
- The MPD has demonstrated **long-term continuous operation** (> 1 year).

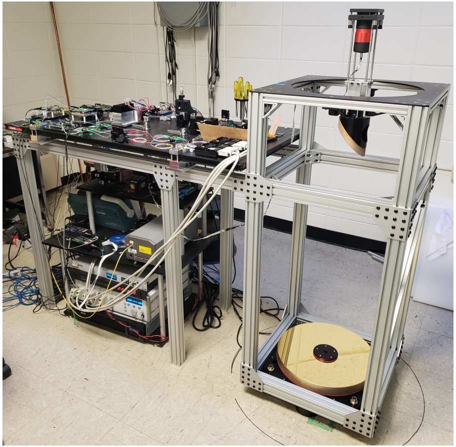

MPD instrument at MSU.

- The MPD's diode-laser-based design is **cost-effective** and enables **eye-safe** operation with a class 1M designation.
- The MPD has demonstrated **long-term continuous operation** (> 1 year).
- The flexible MPD architecture can be adapted to measure **water vapor**, **temperature**, and quantitative **aerosol backscatter** profiles.

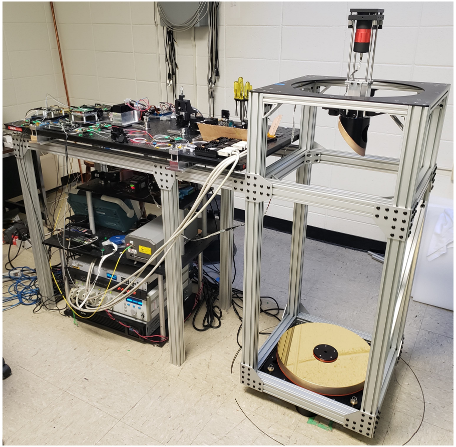

MPD instrument at MSU.

Previous Work: The MicroPulse Differential Absorption Lidar (MPD)

- The MPD's diode-laser-based design is **cost-effective** and enables **eye-safe** operation with a class 1M designation.
- The MPD has demonstrated **long-term continuous operation** (> 1 year).
- The flexible MPD architecture can be adapted to measure **water vapor**, **temperature**, and quantitative **aerosol backscatter** profiles.
- **The MPD design will be adapted to create a Doppler wind lidar instrument.**

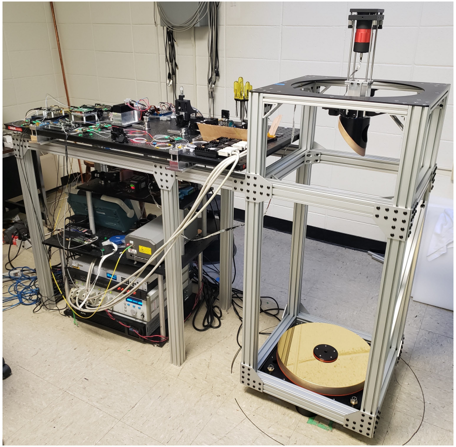

MPD instrument at MSU.

Design Criteria for an MPD-based DWL

Design Criteria for an MPD-based DWL

1. The wavelength must be between 700 nm and 1100 nm.

Design Criteria for an MPD-based DWL

1. The wavelength must be between 700 nm and 1100 nm.

2. The wavelength must not be the same as the other MPD wavelengths (i.e., 770 and 828 nm.)

Design Criteria for an MPD-based DWL

1. The wavelength must be between 700 nm and 1100 nm.

2. The wavelength must not be the same as the other MPD wavelengths (i.e., 770 and 828 nm.)

3. The lidar must use a filter technique (e.g., double-edge etalon and atomic vapor filter edge.)

The Diode-Laser-Based (DLB) Direct-Detection Doppler Wind Lidar (DWL)

- The DLB direct-detection DWL will combine the double-edge technique and the High Spectral Resolution Lidar (HSRL) technique to retrieve vertical wind speeds and the backscatter ratio.

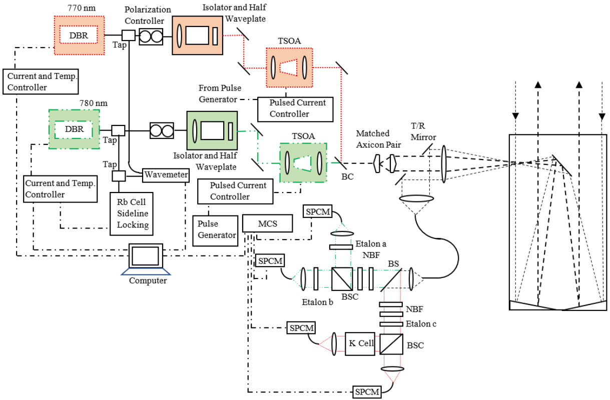

K. Repasky et al. JTech 39, 1655-1668 (2022)
doi:10.1175/JTECH-D-22-0001.1

The Double-Edge Technique

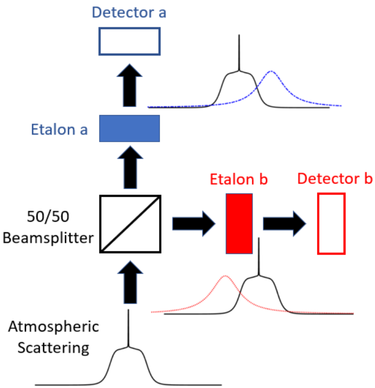

Double-Edge Receiver Block Diagram

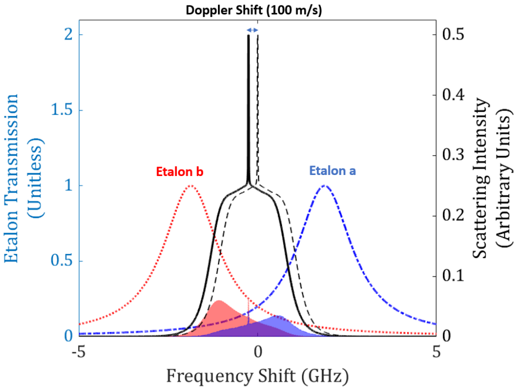

The Double-Edge Technique

The Double-Edge Technique

The Doppler shift can be retrieved numerically from the double-edge equation.

$$\frac{N_a(r) - N_b(r)}{N_a(r) + N_b(r)} = \frac{[\boxed{B(r)} - 1]\Big(\eta_a T_{e,a}(f = f_0 + \boxed{\Delta f(r)}) - \eta_b T_{e,b}(f = f_0 + \boxed{\Delta f(r)})\Big) + \int g(r, f_0 + \boxed{\Delta f(r)}, f)\Big(\eta_a T_{e,a}(f) - \eta_b T_{e,b}(f)\Big)df}{[\boxed{B(r)} - 1]\Big(\eta_a T_{e,a}(f = f_0 + \boxed{\Delta f(r)}) + \eta_b T_{e,b}(f = f_0 + \boxed{\Delta f(r)})\Big) + \int g(r, f_0 + \boxed{\Delta f(r)}, f)\Big(\eta_a T_{e,a}(f) + \eta_b T_{e,b}(f)\Big)df}$$

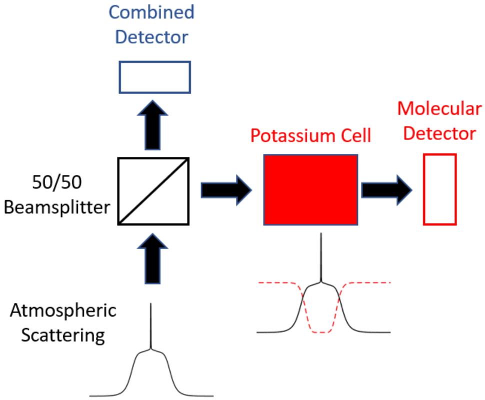

HSRL Receiver Block Diagram

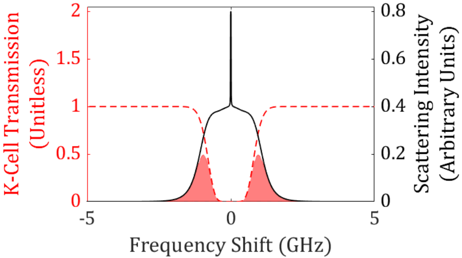

The HSRL Technique

The High Spectral Resolution Lidar (HSRL) Technique

The backscatter ratio can be found algebraically from the HSRL equation.

$$B(r) = 1 + \left(\frac{N_m(r)\eta_c C_{mc}(r) - N_c(r)\eta_m C_{mm}(r)}{N_c(r)\eta_m C_{am} - N_m(r)\eta_c C_{ac}} \right)$$

The DLB Direct-Detection DWL

The first prototype for the DLB Direct-Detection DWL will be a stand-alone instrument and will use the backscatter ratio retrieved by a different lidar.

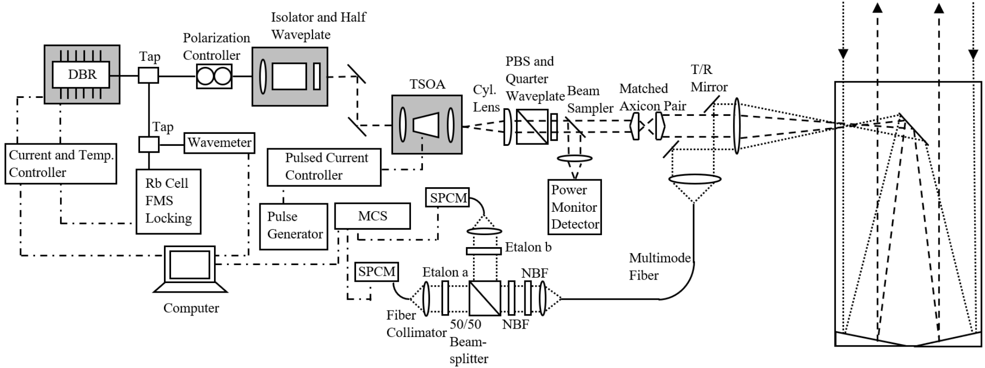

Schematic of the Diode-Laser-Baser Doppler Wind Lidar (DLB-DWL).

The DLB Direct-Detection DWL

The first prototype for the DLB Direct-Detection DWL will be a stand-alone instrument and will use the backscatter ratio retrieved by a different lidar.

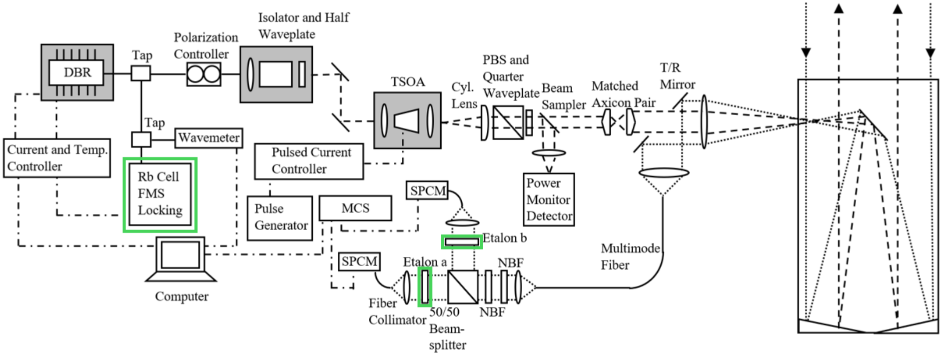

Schematic of the Diode-Laser-Baser Doppler Wind Lidar (DLB-DWL).

Transmitter	**Specification**	**Narrowband Filters**	
Wavelength	780 nm	Interference Filter Bandwidth	750 pm
Linewidth	< 2 MHz	Effective Filter bandwidth	40 pm
Pulse Energy	5 µJ	**Receiver**	**Specification**
Pulse Duration	1 µs	Outer (Inner) Diameter	40.6 cm (20.3 cm)
Pulse Repetition Rate	10 kHz	Area	970 cm^2
Spectral Purity	> 99.5%	Field of View	115 µrad
Laser Divergence	60 µrad	Receiver Efficiency	10%
Etalons		Unambiguous Range	15 km
Free Spectral Range	122 pm	**Detectors**	SPCM
Finesse	20	Quantum Efficiency	50 %
Beam Divergence at Etalon	<2.5 mrad	Dark Count Rate	200 counts s^{-1}
		Dead Time	50 ns

The O_2 Differential Absorption Lidar (DIAL) and HSRL

The O_2 DIAL and HSRL can retrieve the backscatter ratio at 770 nm using a Potassium atomic vapor cell as a filter.

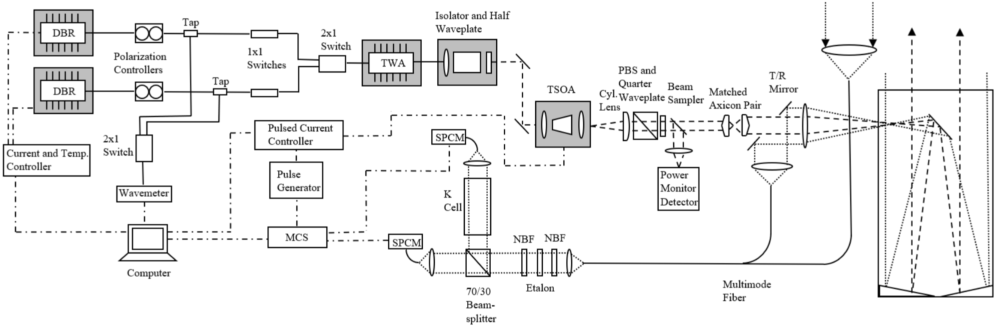

Schematic of the O_2 DIAL and HSRL.

Error Analysis

An error analysis was modeled to understand the efficacy of retrieving wind speeds with this instrument (Repasky et al. 2022). It was found that the vertical wind speed can be retrieved with an accuracy of **0.63 $\frac{m}{s}$ from 0.5-4 km for a 5-minute averaging time and a 150-m range resolution.**

Error Source	Error (m/s)	Contribution to total error
Poisson noise	0.33	27.3%
Laser stability	0.20	10.0%
Etalon stability	0.49	60.1%
Uncertainty in the backscatter ratio	0.02	0.1%
Uncertainty in the atmospheric temperature and pressure	0.10	2.5%
Total error (added in quadrature)	0.63	

DLB Direct-Detection DWL Measurement Niche

The DLB Direct-Detection DWL can serve as a low-cost instrument that can profile the PBL and the lower free troposphere.

Other Direct Detection DWLs (e.g., TWiLiTE, OAWL)	DLB Direct-Detection DWL	Heterodyne DWLs (e.g., Leosphere-Vaisala WindCube)
Sophisticated research instruments	Cost-effective	Cost-effective and commercially-available
Can profile within the aerosol-dense PBL and/or the aerosol-sparse free troposphere depending on the interferometer.	Can profile within the aerosol-dense PBL and the aerosol-sparse free troposphere.	Can only profile within the aerosol-dense PBL.
High-powered solid-state lasers (e.g., 355, 532, 1064 nm)	Near-infrared diode lasers (780 nm)	Shortwave infrared diode lasers (1540 nm)

Statement of Objectives

- **Objective 1 (Main Objective):** Develop and demonstrate a direct-detection DWL system for vertical wind profiling in the lower atmosphere based on the DLB MPD architecture.

- **Objective 1 (Main Objective):** Develop and demonstrate a direct-detection DWL system for vertical wind profiling in the lower atmosphere based on the DLB MPD architecture.
- **Objective 2:** Develop technologies for advancing DLB lidar.

Statement of Objectives

- **Objective 1 (Main Objective):** Develop and demonstrate a direct-detection DWL system for vertical wind profiling in the lower atmosphere based on the DLB MPD architecture.
- **Objective 2:** Develop technologies for advancing DLB lidar.
- **Objective 3:** Demonstrate scientific research capabilities by observing mixing heights with the DLB direct-detection DWL.

Introduction to Completed Work

Introduction to Completed Work

- **Laser Frequency Stabilization** — Completed.

Introduction to Completed Work

- **Laser Frequency Stabilization** — Completed.
- **Laser Transmitter Assembly** — In Progress.

Introduction to Completed Work

- **Laser Frequency Stabilization** — Completed.
- **Laser Transmitter Assembly** — In Progress.
- **Etalon Temperature Stabilization** — Nearly Completed.

Introduction to Completed Work

- **Laser Frequency Stabilization** — Completed.
- **Laser Transmitter Assembly** — In Progress.
- **Etalon Temperature Stabilization** — Nearly Completed.
- **Lidar Receiver Assembly** — In Progress.

Laser Stabilization: Frequency Modulation Spectroscopy (FMS) 20

FMS can be used to measure the derivative of an absorption feature.

$$Error\ Signal \propto \frac{dTransmission}{d\lambda}$$

Single-Pass Rubidium Vapor Cell Absorption Spectrum

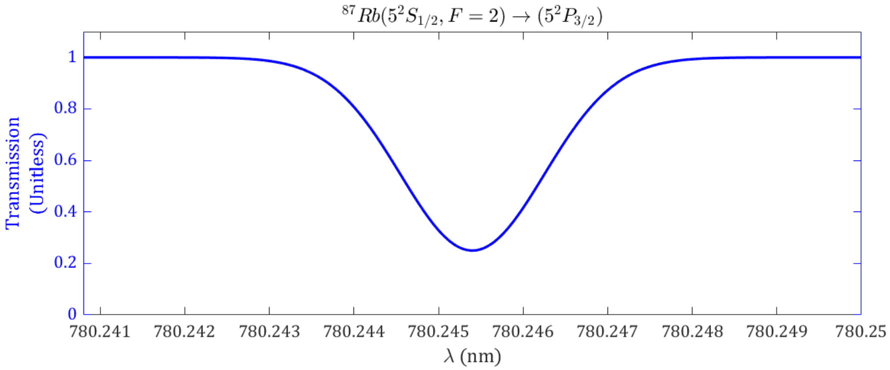

Double-Pass Rubidium Vapor Cell Absorption Spectrum

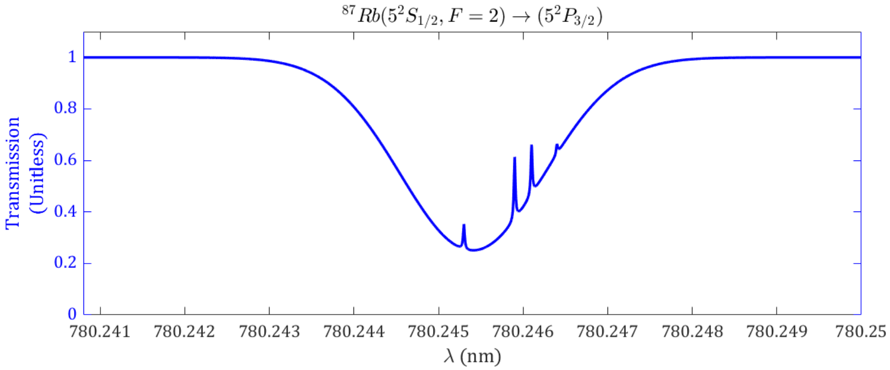

Double-Pass Rubidium Vapor Cell Absorption Spectrum

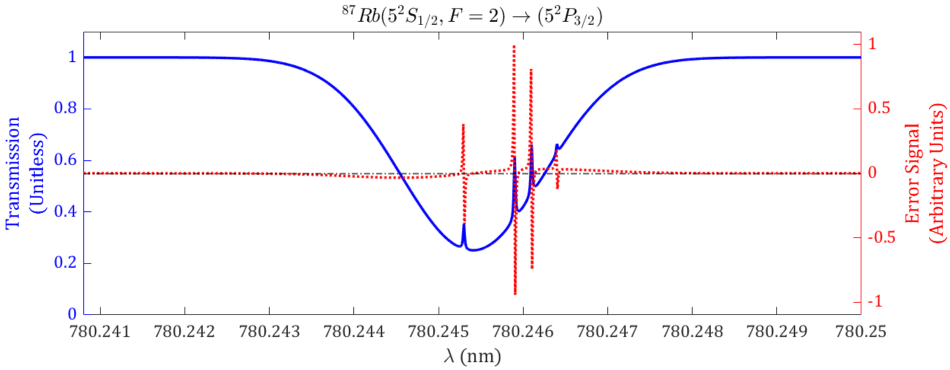

$$\textit{Error Signal} \propto \frac{d\,\textit{Transmission}}{d\lambda}$$

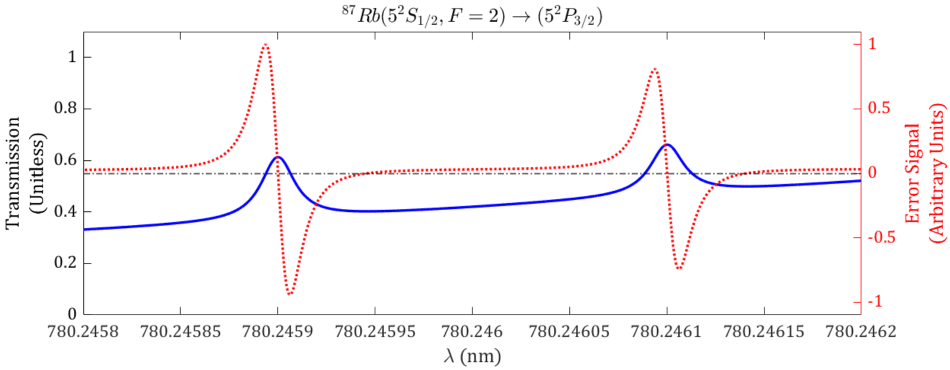

Laser Stabilization: Control Loop

The laser is stabilized to a hyperfine transition of the ^{87}Rb D2 line using frequency modulation spectroscopy **(FMS)** and saturated absorption spectroscopy.

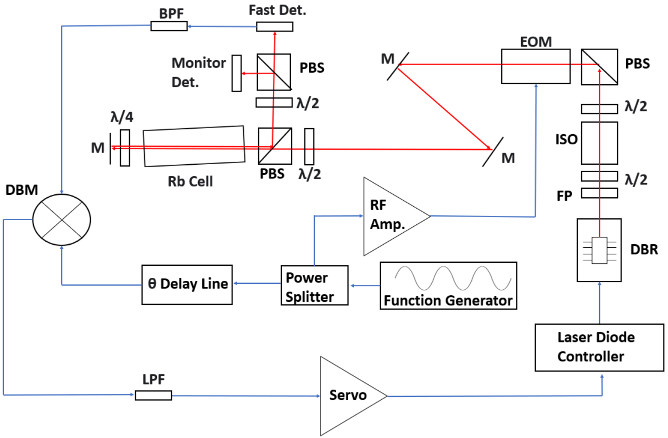

Laser Frequency Stabilization Loop Block Diagram.

Laser Stabilization: Testing and Results

Laser Stabilization: Testing and Results

Two lasers were stabilized to adjacent saturated absorption lines for 48 hours.

Two lasers were stabilized to adjacent saturated absorption lines for 48 hours. The beat note had a stability of 97 kHz, **indicating a laser stability of 69 kHz ($0.027\ \frac{m}{s}$)**.

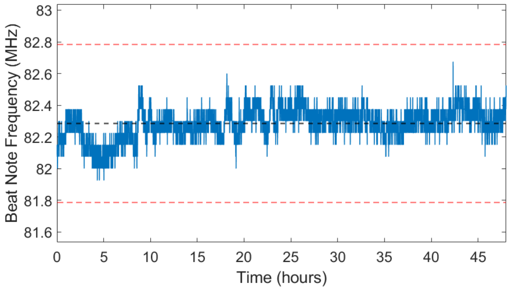

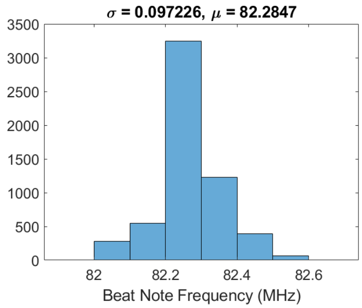

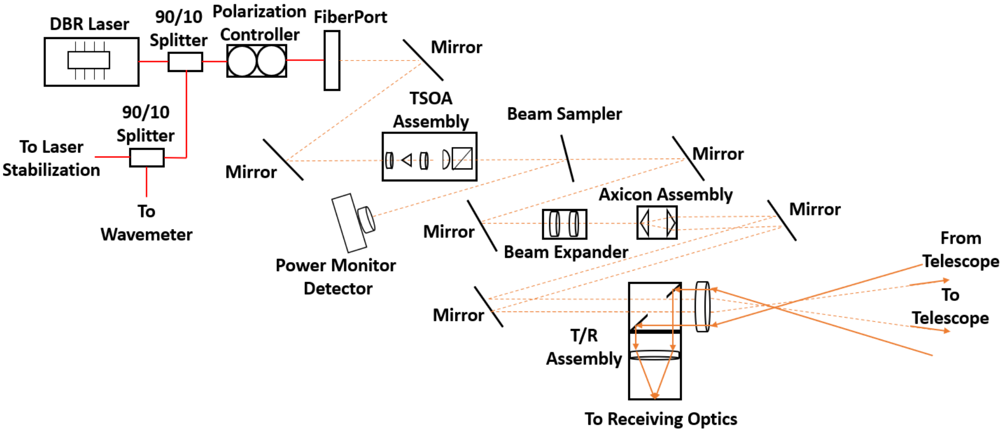

Laser Transmitter Block Diagram.

Laser Transmitter

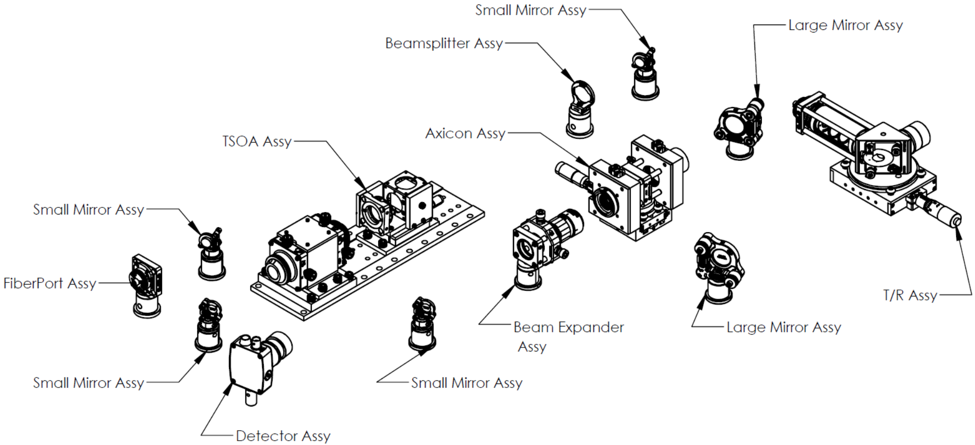

Laser Transmitter SolidWorks Drawing.

Laser Transmitter continued

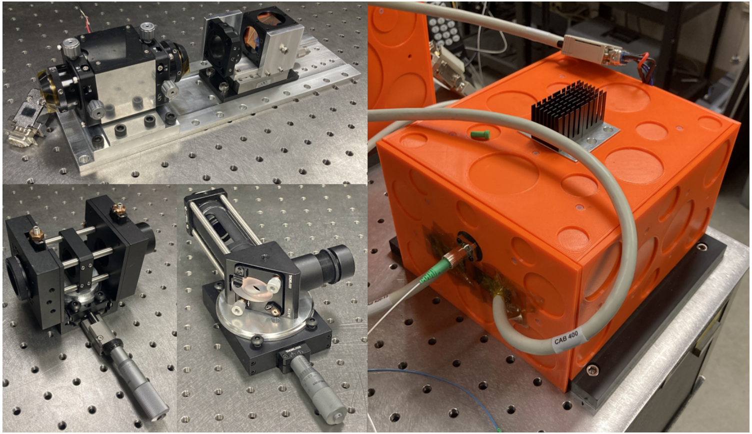

Top Left: TSOA Assembly. Bottom Left: Axicon Assembly. Bottom Center: T/R Assembly. Right: Laser Enclosure.

Fused Silica Etalons

Fused Silica Etalons

- Unlike other double-edge lidars, **our system will use fused silica etalons** as edge filters instead of actively locked Fabry-Perot cavities.

Fused Silica Etalons

- Unlike other double-edge lidars, **our system will use fused silica etalons** as edge filters instead of actively locked Fabry-Perot cavities.

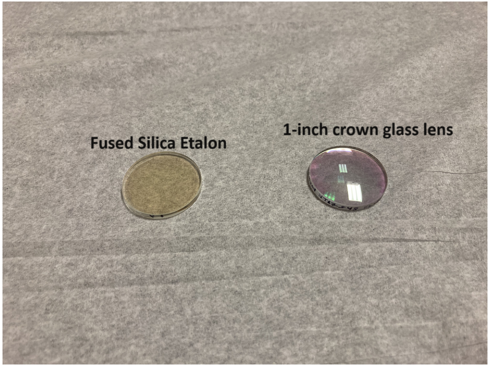

Fused Silica Etalons

- Unlike other double-edge lidars, **our system will use fused silica etalons** as edge filters instead of actively locked Fabry-Perot cavities.

- A fused silica etalon is easy to use and optomechanically stable, but requires greater temperature stability (**In our case, <5mK**).

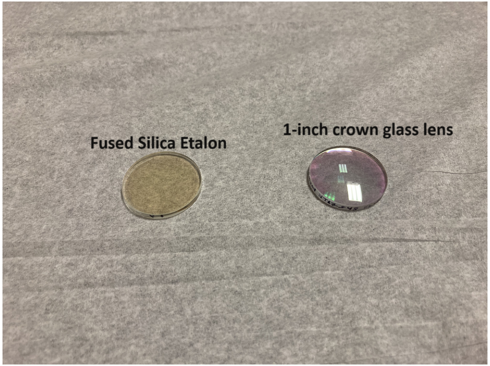

The temperature stability will be achieved with 2 layers of active temperature stabilization.

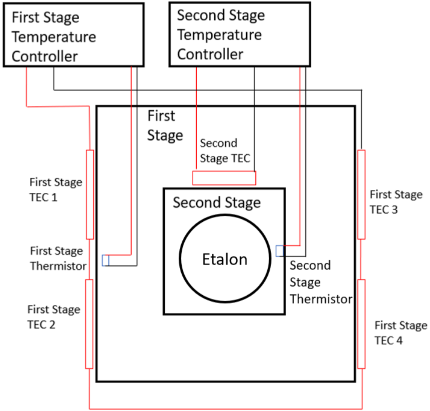

Block diagram of the temperature-stabilized etalon mount.

Temperature-Stabilized Etalon Mount

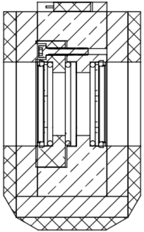

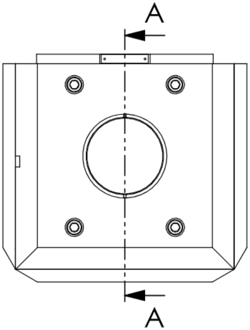

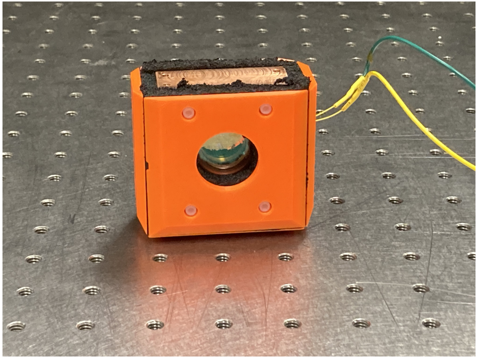

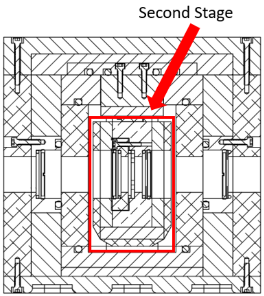

Second Stage

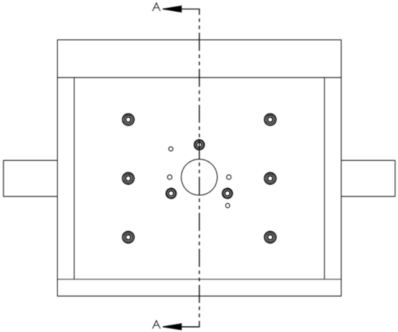

A
A

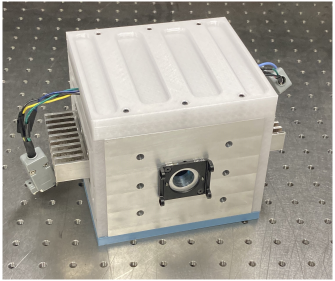

Temperature-Stabilized Etalon

The temperature stability of the etalon was monitored by stabilizing the laser, tuning the etalon so that the sideline was at the laser frequency, and monitoring the transmission.

$$\frac{\Delta\lambda}{\Delta(Temperature)} = 0.508\ \frac{pm}{mK}$$

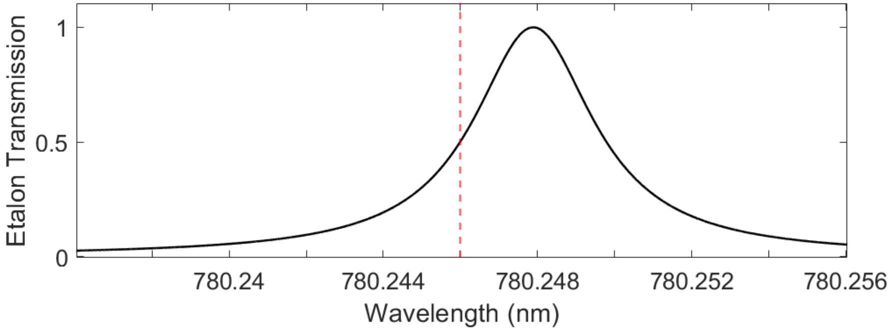

Temperature-Stabilized Etalon

The best performance was a **temperature stability of 1.15 mK (.113 $\frac{m}{s}$) for 96 hours.**

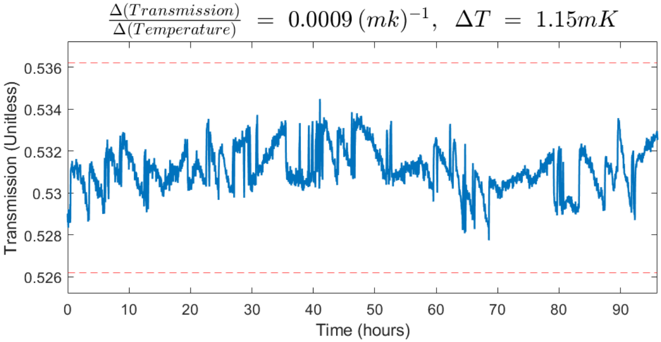

Temperature-Stabilized Etalon

In general, the temperature-stabilized etalon mount can maintain a **temperature stability of 2 mK (.196 $\frac{m}{s}$) for 1-hour time periods and 10 mK for (.980 $\frac{m}{s}$) 24-hour time periods.**

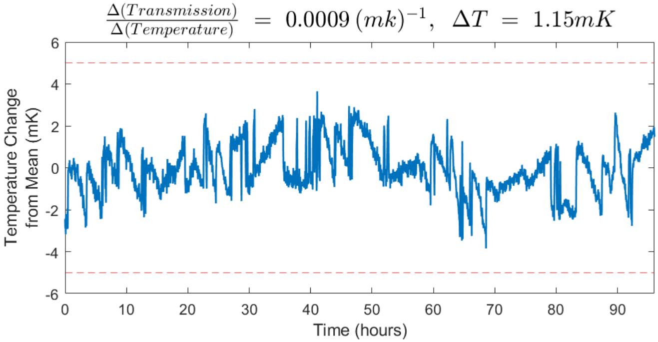

Lidar Receiver

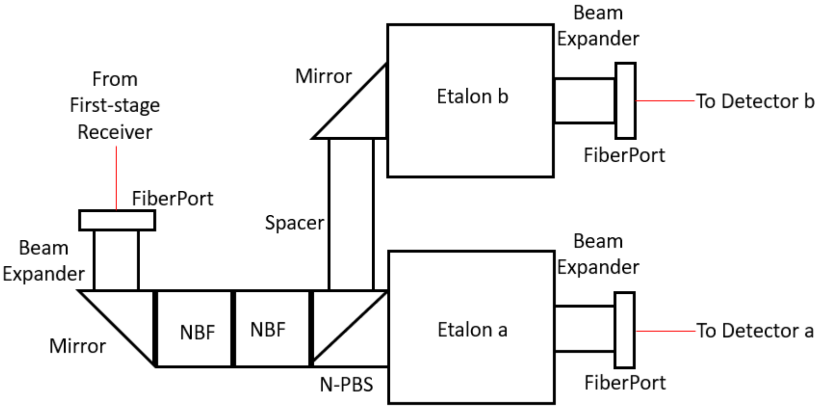

Lidar Receiver Block Diagram.

Lidar Receiver

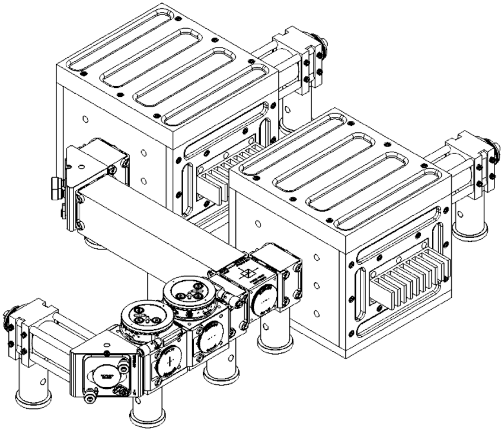

Lidar Receiver SolidWorks Drawing.

Lidar Receiver

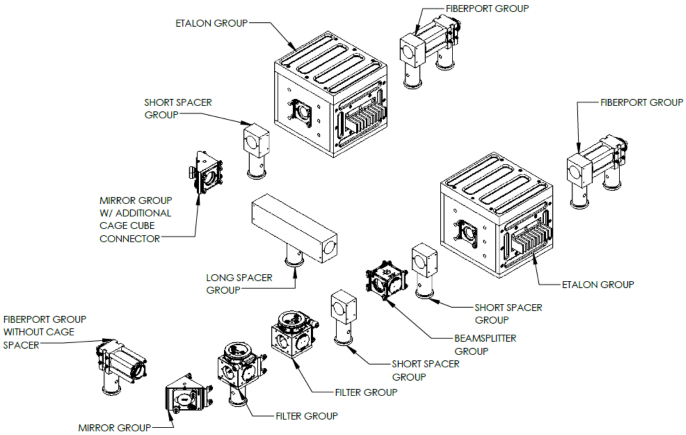

Lidar Receiver SolidWorks Drawing.

Lidar Receiver

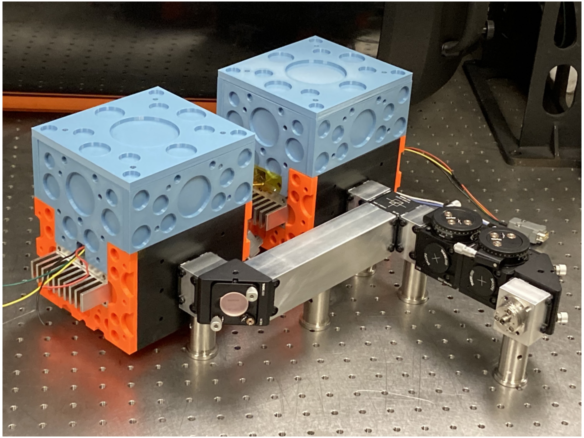

Lidar Receiver Photo.

Updated Error Analysis

The error analysis from (Repasky et al. 2022) was updated with the new laser and etalon stabilities and it was found that the vertical wind speed can be retrieved with an accuracy of **0.40 $\frac{m}{s}$ from 0.5-4 km for a 5-minute averaging time and a 150-m range resolution.**

Error Source	Error (m/s)	Contribution to total error
Poisson noise	0.33	67.7%
Laser stability	0.04	1.0%
Etalon stability	0.20	24.9%
Uncertainty in the backscatter ratio	0.02	0.2%
Uncertainty in the atmospheric temperature and pressure	0.10	6.2%
Total error (added in quadrature)	0.40	

Introduction to Research Plan

Introduction to Research Plan

- **Phase 1:** Hardware Assembly, Characterization, and Alignment (March 2024 - June 2024)

- **Phase 1:** Hardware Assembly, Characterization, and Alignment (March 2024 - June 2024)
- **Phase 2:** Control Software and Retrieval Algorithm Development (July 2024 - September 2025)

Introduction to Research Plan

- **Phase 1:** Hardware Assembly, Characterization, and Alignment (March 2024 - June 2024)
- **Phase 2:** Control Software and Retrieval Algorithm Development (July 2024 - September 2025)
- **Phase 3:** Testing, Troubleshooting, Horizontal Validation, and Mixing Height Retrievals (September 2025 - December 2025)

Transmitter Assembly and Testing (March 2024 - May 2024)

The transmitter will be assembled and aligned. Spectral purity measurements of the TSOA output will be taken with an optical spectrum analyzer.

The transmitter will be assembled and aligned. Spectral purity measurements of the TSOA output will be taken with an optical spectrum analyzer.

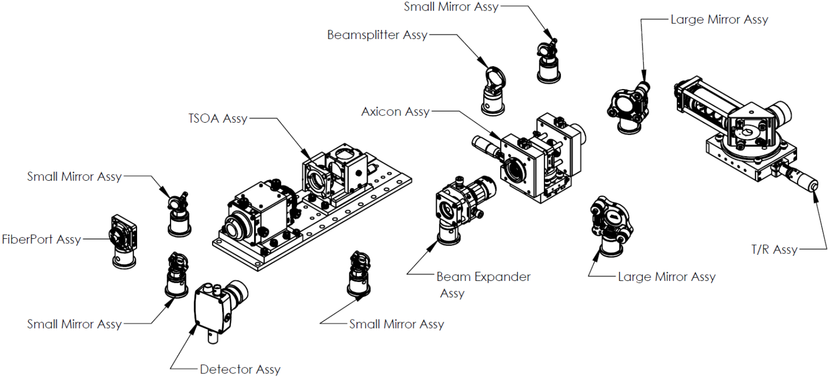

The transmitter will be assembled and aligned. Spectral purity measurements of the TSOA output will be taken with an optical spectrum analyzer.

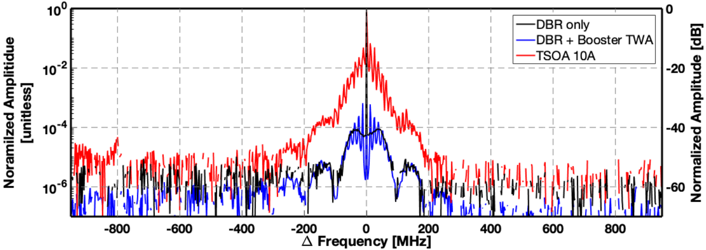

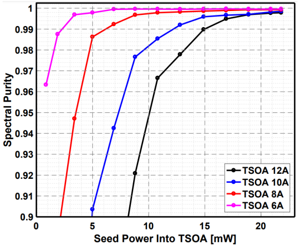

S. Spuler et al., Atmos. Meas. Tech., 14, 4593–4616, 2021, doi:10.5194/amt-14-4593-2021.

Receiver Assembly and Alignment (March 2024 - May 2024)

The receiver will be assembled and aligned, and the transmission of the etalons will be characterized.

Receiver Assembly and Alignment (March 2024 - May 2024)

The receiver will be assembled and aligned, and the transmission of the etalons will be characterized.

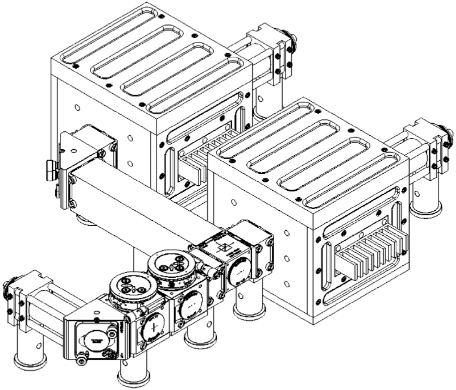

The receiver will be assembled and aligned, and the transmission of the etalons will be characterized.

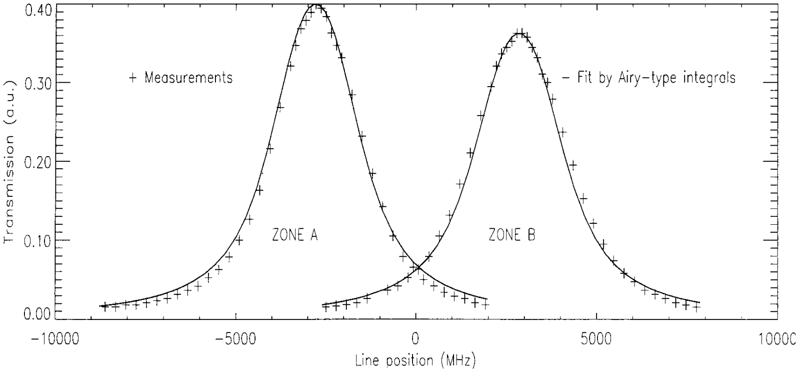

C. Souprayen et al., Appl. Opt., 38, 2422-2431, 1999, doi:10.1364/AO.38.002422.

Lidar Assembly and Alignment (May 2024 - June 2024)

The transmitter and the receiver will be aligned with the telescope in a roofport-equipped laboratory.

Lidar Assembly and Alignment (May 2024 - June 2024)

The transmitter and the receiver will be aligned with the telescope in a roofport-equipped laboratory.

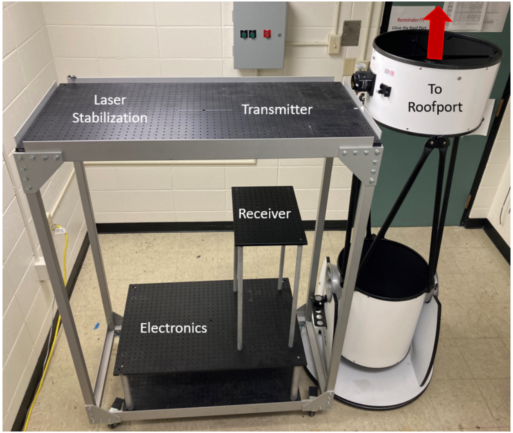

Data Acquisition Program (July 2024 - September 2024)

The instrument will be controlled by a LabVIEW program. This program will have the following functions:

Data Acquisition Program (July 2024 - September 2024)

The instrument will be controlled by a LabVIEW program. This program will have the following functions:

- Continuously collect data and store it as netCDF files.

Data Acquisition Program (July 2024 - September 2024)

The instrument will be controlled by a LabVIEW program. This program will have the following functions:

- Continuously collect data and store it as netCDF files.
- Control the temperature of the etalons.

Data Acquisition Program (July 2024 - September 2024)

The instrument will be controlled by a LabVIEW program. This program will have the following functions:

- Continuously collect data and store it as netCDF files.
- Control the temperature of the etalons.
- Monitor whether or not the laser is stabilized.

Data Acquisition Program (July 2024 - September 2024)

The instrument will be controlled by a LabVIEW program. This program will have the following functions:

- Continuously collect data and store it as netCDF files.
- Control the temperature of the etalons.
- Monitor whether or not the laser is stabilized.
- Collect background photon count rates.

The instrument will be controlled by a LabVIEW program. This program will have the following functions:

- Continuously collect data and store it as netCDF files.
- Control the temperature of the etalons.
- Monitor whether or not the laser is stabilized.
- Collect background photon count rates.
- Collect calibration scans for the etalon transmission.

Data Acquisition Program (July 2024 - September 2024)

The instrument will be controlled by a LabVIEW program. This program will have the following functions:

- Continuously collect data and store it as netCDF files.
- Control the temperature of the etalons.
- Monitor whether or not the laser is stabilized.
- Collect background photon count rates.
- Collect calibration scans for the etalon transmission.
- Measure biases due to etalon drift.

Calibration Program (July 2024 - September 2024)

To calibrate the etalons, the TSOA will be turned off and a shutter will be closed at the focal point of the telescope, reflecting a tiny amount of light at the laser wavelength into the receiver. The laser will not be stabilized and the wavelength will be scanned over the etalon transmission spectra.

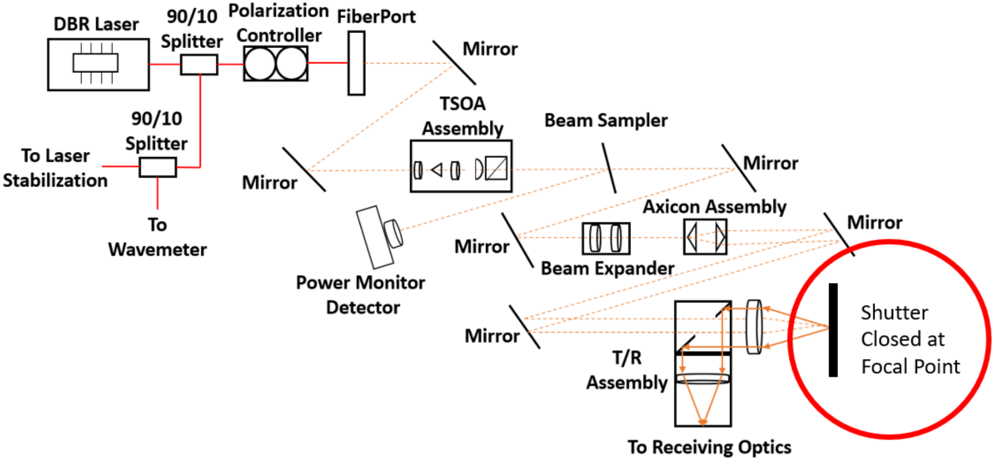
DBR Laser
90/10 Splitter
Polarization Controller
FiberPort
Mirror
TSOA Assembly
Beam Sampler
90/10 Splitter
To Laser Stabilization
Mirror
Mirror
To Wavemeter
Axicon Assembly
Mirror
Mirror
Beam Expander
Power Monitor Detector
Shutter Closed at Focal Point
Mirror
T/R Assembly
To Receiving Optics

Bias Measurement (July 2024 - September 2024)

To monitor biases, the TSOA will be turned off and a shutter will be closed at the focal point of the telescope, reflecting a tiny amount of light at the laser wavelength into the second stage receiver. The laser will be stabilized.

Bias Measurement (July 2024 - September 2024)

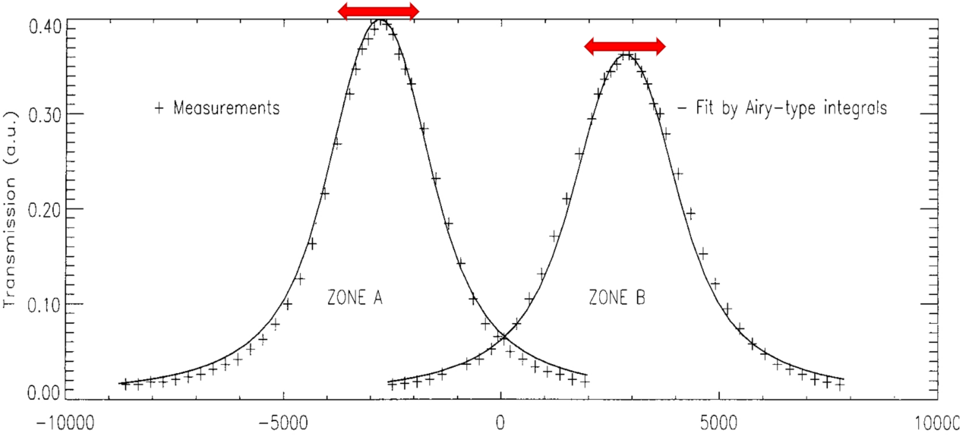

C. Souprayen et al., Appl. Opt., 38, 2422-2431, 1999, doi:10.1364/AO.38.002422.

Retrieval Program (October 2024 - August 2025)

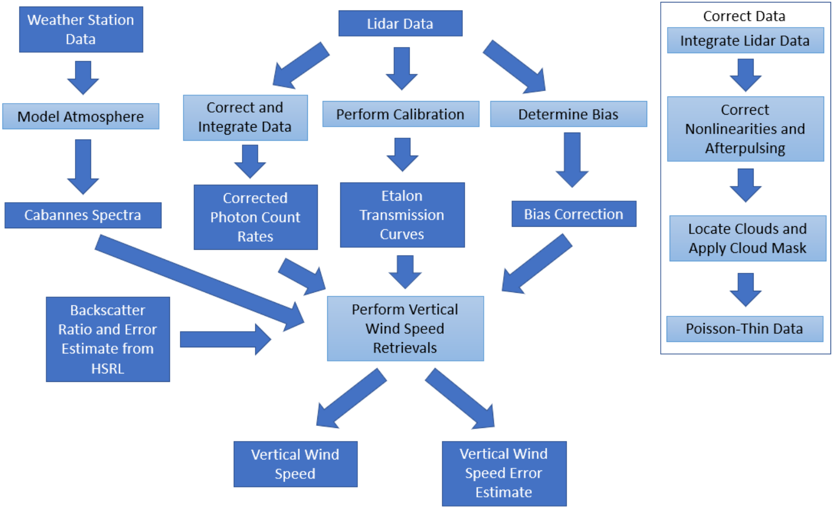

Troubleshooting, Testing, Horizontal Validation (September 2025-December 2025)

Troubleshooting, Testing, Horizontal Validation (September 2025-December 2025)

- Time has been preallocated to solve unknown issues.

- Time has been preallocated to solve unknown issues.
- Once the wind speed retrieved by the lidar appears realistic, I will move to horizontal validation.

Troubleshooting, Testing, Horizontal Validation (September 2025-December 2025)

- Time has been preallocated to solve unknown issues.
- Once the wind speed retrieved by the lidar appears realistic, I will move to horizontal validation.
- The DLB direct-detection DWL will be transmitted horizontally and the retrieved wind speed compared to an anemometer.

Mixing Height Retrievals (September 2025- December 2025)

Mixing Height Retrievals (September 2025- December 2025)

- The mixing height describes the height of turbulent mixing in the atmosphere.

- The mixing height describes the height of turbulent mixing in the atmosphere.
- The mixing height will be retrieved by observing the variance of the vertical velocity.

- The mixing height describes the height of turbulent mixing in the atmosphere.
- The mixing height will be retrieved by observing the variance of the vertical velocity.
- These retrievals will be compared to the HSRL mixing height retrievals.

Mixing Height Retrievals (September 2025- December 2025)

- The mixing height describes the height of turbulent mixing in the atmosphere.
- The mixing height will be retrieved by observing the variance of the vertical velocity.
- These retrievals will be compared to the HSRL mixing height retrievals.

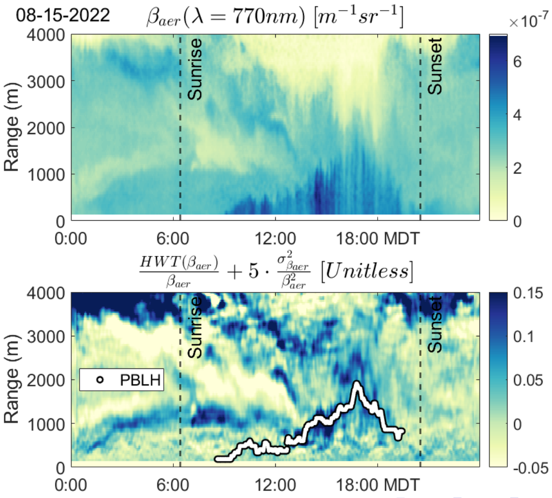

Planned Publications

Planned Publications

1. Demonstration of a Diode-Laser-Based Direct-Detection Doppler Wind Lidar (Mid 2025).

Planned Publications

1. Demonstration of a Diode-Laser-Based Direct-Detection Doppler Wind Lidar (Mid 2025).

2. Design and Demonstration of a Temperature-Stabilized Etalon Enclosure for Double-Edge Wind Lidar (Late 2024/Early 2025).

Planned Publications

1. Demonstration of a Diode-Laser-Based Direct-Detection Doppler Wind Lidar (Mid 2025).
2. Design and Demonstration of a Temperature-Stabilized Etalon Enclosure for Double-Edge Wind Lidar (Late 2024/Early 2025).
3. Mixing Height Retrievals using the Diode-Laser-Based Direct-Detection Doppler Wind Lidar (Late 2025).

Planned Publications

1. Demonstration of a Diode-Laser-Based Direct-Detection Doppler Wind Lidar (Mid 2025).
2. Design and Demonstration of a Temperature-Stabilized Etalon Enclosure for Double-Edge Wind Lidar (Late 2024/Early 2025).
3. Mixing Height Retrievals using the Diode-Laser-Based Direct-Detection Doppler Wind Lidar (Late 2025).
4. Mixing Height Retrievals from the MicroPulse DIAL during the M2HATS Field Experiment (Late 2024/Early 2025).

Conclusions

Conclusions

1. A diode-laser-based direct-detection Doppler wind lidar that combines the double-edge and the high spectral resolution techniques for vertical profiling of vertical wind speeds and the backscatter ratio has been conceptualized.

Conclusions

1. A diode-laser-based direct-detection Doppler wind lidar that combines the double-edge and the high spectral resolution techniques for vertical profiling of vertical wind speeds and the backscatter ratio has been conceptualized.
2. Two necessary subsystems for this instrument, laser frequency stabilization and etalon temperature stabilization have been developed. Work has also commenced on assembling the laser transmitter and lidar receiver.

Conclusions

1. A diode-laser-based direct-detection Doppler wind lidar that combines the double-edge and the high spectral resolution techniques for vertical profiling of vertical wind speeds and the backscatter ratio has been conceptualized.
2. Two necessary subsystems for this instrument, laser frequency stabilization and etalon temperature stabilization have been developed. Work has also commenced on assembling the laser transmitter and lidar receiver.
3. A plan for assembling the instrument, developing the control software and retrieval algorithm, validating the measurements, and retrieving the mixing height has been proposed.

Conclusions

1. A diode-laser-based direct-detection Doppler wind lidar that combines the double-edge and the high spectral resolution techniques for vertical profiling of vertical wind speeds and the backscatter ratio has been conceptualized.
2. Two necessary subsystems for this instrument, laser frequency stabilization and etalon temperature stabilization have been developed. Work has also commenced on assembling the laser transmitter and lidar receiver.
3. A plan for assembling the instrument, developing the control software and retrieval algorithm, validating the measurements, and retrieving the mixing height has been proposed.
4. Developing remote sensing instruments like the diode-laser-based direct-detection Doppler wind lidar is vital for advancing weather forecasting and atmospheric science.

Conclusions

1. A diode-laser-based direct-detection Doppler wind lidar that combines the double-edge and the high spectral resolution techniques for vertical profiling of vertical wind speeds and the backscatter ratio has been conceptualized.
2. Two necessary subsystems for this instrument, laser frequency stabilization and etalon temperature stabilization have been developed. Work has also commenced on assembling the laser transmitter and lidar receiver.
3. A plan for assembling the instrument, developing the control software and retrieval algorithm, validating the measurements, and retrieving the mixing height has been proposed.
4. Developing remote sensing instruments like the diode-laser-based direct-detection Doppler wind lidar is vital for advancing weather forecasting and atmospheric science.

Acknowledgements: This research was supported by the National Science Foundation through grant #1917851.